

Nucleation-limited aggregation in fractal growth

Nai-ben Ming, Mu Wang, and Ru-Wen Peng

Center for Condensed Matter Physics and Radiation Physics, China Center of Advanced Science and Technology (World Laboratory),
P. O. Box 8730, Beijing, People's Republic of China

and National Laboratory of Solid State Microstructures and Department of Physics, Nanjing University,
Nanjing 210008, People's Republic of China*

(Received 22 March 1993)

In situ observation technique is employed to study the fractal growth in a thin isothermal aqueous-solution film of $\text{Ba}(\text{NO}_3)_2$. The micromorphology and the growing process of the fractals have been investigated. The experimental findings provide direct evidence that the fractals are formed by random successive nucleation. A nucleation-limited-aggregation (NLA) model is proposed to describe the fractal growth in our system. A computer simulation using the NLA model is also presented.

PACS number(s): 61.50.Cj, 64.60.Qb, 68.70.+w, 05.40.+j

Pattern formation in a nonequilibrium situation is a subject of increasing interest and has been investigated intensively both in theory and in experiment over the past decade [1,2]. So far, a clear understanding of nonequilibrium growth in a Laplacian field has been achieved [2]. Yet many important questions remain unanswered. For example, it is still an open question whether the fractal is a product of the randomness in the growth process or a result of proliferation of deterministic tip-splitting instability. On the other hand, since the introduction of the diffusion-limited-aggregation (DLA) model by Witten and Sander [3], many efforts have been made to modify the model in order to describe the experiments more accurately. For instance, Uwaha and Saito proposed the finite-density DLA model [4], which describes the aggregates growing from a lattice gas with a nonzero gas density n_g . Unlike the original DLA model, which represents the growth in the low-density limit of the diffusion field, the finite-density DLA demonstrates the growing process with higher driving force. However, in reality, when the growth system is far from equilibrium, i.e., when the driving force becomes extremely high, the nucleation phenomenon is absolutely non-negligible. Will there be fractal aggregates in this situation? If the answer is positive, then what is the growth mechanism of the fractals? The studies on the morphology of the aggregates, especially the *in situ* investigation of the aggregate-growth process, we believe, are specifically important to answer these questions.

In this Brief Report we report the experimental studies on the fractal growth in aqueous-solution film of $\text{Ba}(\text{NO}_3)_2$ with a free surface. The experimental system is the same as that reported previously [5]. A uniform $\text{Ba}(\text{NO}_3)_2$ aqueous-solution film is mounted on a very clean glass substrate. Initial thickness of the film varies from several tens to a hundred micrometers. An evaporation method is employed both to generate high supersaturation for the fractal growth and to compensate for the decrease of solute concentration caused by the fractal growth. Flowing N_2 gas is used to enhance the transportation of water vapor out from the growth chamber. The

relative humidity in the growth chamber is adjusted to 90% and N_2 flow is 1.0 l/min at 25°C. The pressure of the N_2 is kept at 1.0 kg/cm². Initial concentration of the aqueous solution is 9.3% by weight, which is the saturated concentration at 25°C. The temperature in the isothermal growth chamber, which is several degrees higher than the room temperature, is controlled at 25.00 ± 0.05 °C by the built-in heating system. The fractal growth is monitored by a microscope (Leitz, Orthoplan-pol) with video and camera recording systems.

The typical observed fractal pattern is shown in Fig. 1(a). The supersaturation for the fractal growth, $\sigma = (C - C_0)/C_0$, is about 3.0–4.0, where C_0 is the saturated concentration at the temperature at which the experiment is performed. This supersaturation is much higher than that for the crystal growth in usual cases, and is about one order of magnitude higher than the critical supersaturation for nucleation, as we will discuss below. This means that the fractal growth is far from equilibrium in our case. Meanwhile, the thickness of the aqueous solution film is less than 40 μm . The dimension of the pattern shown in Fig. 1(a) is determined by digitizing the image and using the sand-box method. Figure 1(b) indicates that the fractal dimension is 1.76 ± 0.03 . The density-density correlation function of the same pattern is illustrated in Fig. 1(c), where the linear region indicates the scale invariance of the pattern.

The micromorphology of the fractal pattern viewed under a scanning electron microscope (SEM) is shown in Fig. 2(a). Instead of a single crystal, the fractal is an assembly for small crystals with their size varying from one to several micrometers. To confirm the microstructure of the fractal, we etch the fractal slightly. Figure 2(b) shows the same fractal as that shown in Fig. 1(a), which has been deliquesced in open atmosphere for several days. Evidently the branches of the fractal consist of many small crystals. It is well known that the etching rate at the grain boundary is much higher, so the connected crystals in the branch of the fractals are all separated after being etched. Figure 3 shows the fractal-growth process. The time interval between the two successive

photos is about 0.4 s. As indicated by the arrows, an additional small crystal has been generated in front of the tip of the fractal branch between successive pictures. Figure 3 not only confirms that the fractal is composed of small crystals, but also indicates that random successive nucleation is responsible for the fractal growth in this system.

Figures 1(a) and 3 also show that the overall morphology of the fractal depends on the positions where the new nuclei are randomly stimulated in front of the tip of the fractals. If only one nucleus is stimulated each time, as indicated by the arrow in Fig. 3, the branch of the fractals will grow forward in a broken line; if several nuclei are

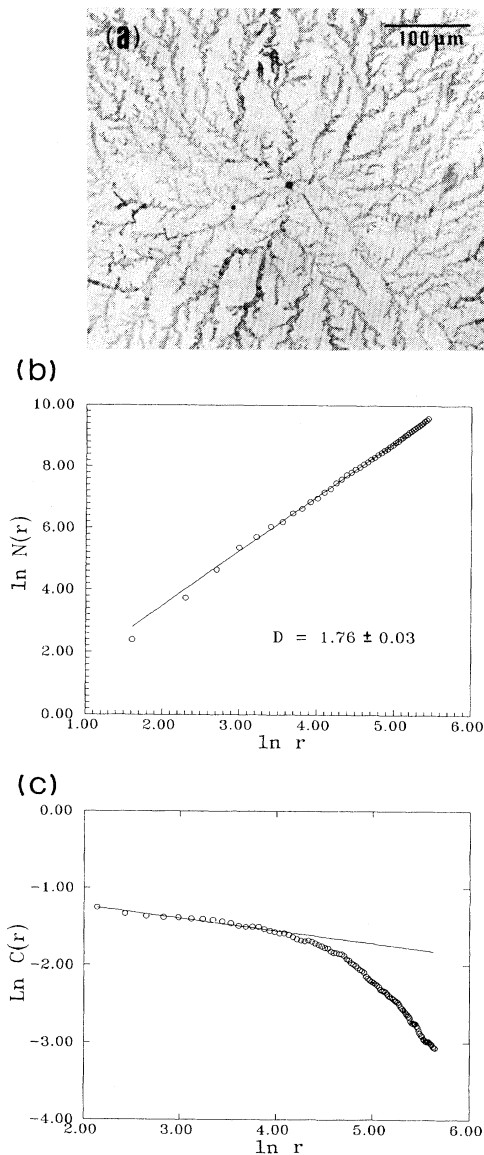


FIG. 1. (a) Typical fractal pattern observed in the experiments. (b) The plot of $\ln N(r)$ vs $\ln r$ to determine Hausdorff dimension of the pattern, where $N(r)$ stands for the area occupied by the fractal within a circle of radius r . (c) The plot to show the density-density correlation function of the cluster shown in (a).

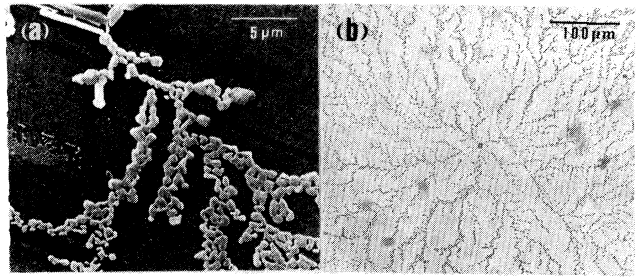


FIG. 2. (a) The fractal branches viewed under a scanning electron microscope. Clearly, the fractal is composed of small crystals. (b) The fractal pattern that has been deliquesced in open atmosphere for several days. The fractal is the same as that shown in Fig. 1(a).

stimulated synchronously, then branch splitting may occur. The number of nuclei that are stimulated each time, and hence the splitting of the branches, decides the morphology of the fractal. Figures 1(a) and 2(a) show that bipartite and tripartite branch splitting are most often seen.

The *in situ* observation shows that the stimulated nuclei are generated around the growing small crystals and usually one to several micrometers away. In our highly supersaturated growth system, nucleation is sensitive to disturbance. In the thin-film growth system with a free surface, there exists a surface-tension gradient (STG) corresponding to the concentration boundary layer at the tip of the growing fractal. During the growth, the STG periodically changes because of the competition of solute depletion within the concentration boundary layer (due to the fractal growth) and solute supply from outside the boundary layer [5]. In a thin-film-growth system, mass

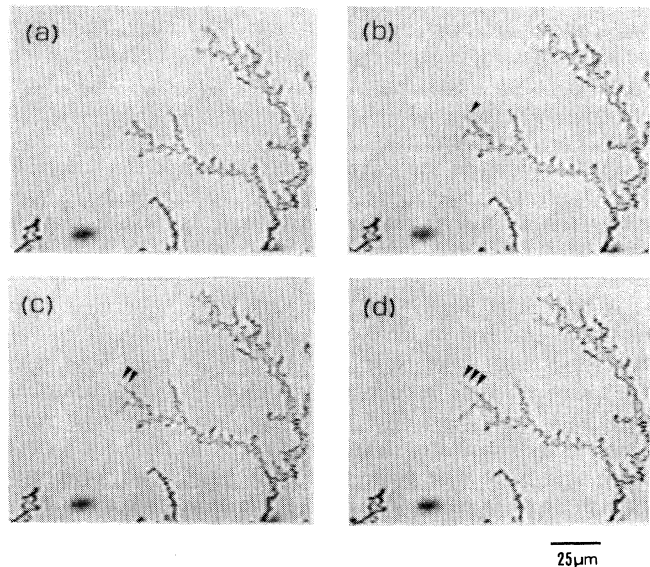


FIG. 3. The fractal-growth process. As indicated by the arrows, successive photos show an additional small crystal generated in front of the tip of the branch. The time interval of two successive photos is about 0.4 s.

transfer is limited by the film thickness, so the role of this competition is more evident. The periodic changes of the STG are responsible for the radially transmitting surface-tension wave (STW). The STW propagates away from the growing small crystal at the tip of the fractal and plays the role of mechanical disturbance [6]. Therefore the newly nucleated small crystal is actually the source of the radially propagating mechanical disturbance during its growth. This disturbance is responsible for stimulating the next generation of nuclei randomly. In this way the random successive nucleation process is self-perpetuating. It is helpful to understand the random successive nucleation process by checking the concentration field around a growing fractal tip. The average fractal growth rate V is about $5 \mu\text{m/s}$ according to Fig. 3. So the width of the concentration boundary layer, which is expressed approximately as $l = D/V$, is about $40 \mu\text{m}$, where D is the diffusion constant and is of the order of $10^{-6} \text{ cm}^2/\text{s}$ for most aqueous-solution growth. The specific surface free energy of the solid-liquid interface between the nucleus and the aqueous solution, γ_{sl} , is about $5 \times 10^{-2} \text{ J/m}^2$, according to the empirical expression given by Söhnel [7]. So the critical supersaturation for nucleation [8,9] σ^* , which is expressed as $\sigma^* = \exp[2\gamma_{sl}\Omega_S/(kTr^*)] - 1$, is about 0.16, where Ω_S is the volume of the crystal atom, r^* is the critical radius of the nucleus, which is taken to be 200 \AA in our case, and k and T are the Boltzman constant and temperature, respectively. Considering the average supersaturation outside the concentration boundary layer and the exponential concentration distribution around the small crystal, as well as the size of the boundary layer, we find that the critical supersaturation for nucleation just corresponds to a position about $1.6 \mu\text{m}$ away from the small crystal. This means that the nuclei can be easily stimulated one micrometer away from the growing small crystal by the disturbance, which is consistent with the experimental result [Fig. 2(a)]. When a nucleus is stimulated, the growth of the nucleus again builds up a concentration boundary layer; hence the disturbance is again generated and transmits away from the growing nucleus. This disturbance stimulates a new generation of nuclei one to several micrometers away from the growing small crystal, at the place where the concentration exceeds the critical concentration for nucleation. We suggest that this self-sustained random successive nucleation process is responsible for the formation of the fractal pattern in our system.

Obviously the fractal growth in our case is limited by the random nucleation process in aqueous-solution film; for this reason, we call it nucleation-limited aggregation (NLA). Using the NLA model, we simulate the fractal growth by the Monte Carlo method. The method is summarized as follows: Initially, we choose a central seed crystal. Surrounding the seed on a circle of radius L , which stands for the distance between the growing small crystal and the position where the supersaturation exceeds the critical value for nucleation, the positions of the second generation of small crystals are randomly chosen, with the restriction that the distance between the neighboring small crystals within the same generation

should be greater than a given value λ . λ actually decides the maximum number of the stimulated nuclei that could grow each time and is a parameter describing the influence of diffusion field on the pattern formation. After the appearance and growth of the second generation of small crystals, the third generation of nuclei are stimulated around the second-generation ones in a similar manner, and the process goes on *ad infinitum*. The morphology of the fractals is closely related to λ . As λ decreases, the growth pattern becomes more and more compact. Considering the screen effect, $r(n+1) > r(n)$ should hold, where $r(n)$ stands for the distance between the n th generation of the stimulated crystals and the seed crystals. We performed the simulation on a Vax 8550 computer. Figure 4(a) illustrates the typical fractal aggregate with 3000 particles. The Hausdorff dimension of the pattern is 1.74 ± 0.02 . The density-density correlation function as shown in Fig. 4(b), the feature of scale invariance of the cluster can be clearly seen.

Now the question arises, what is the difference between the NLA model and the DLA model? The growth probability of the DLA at a perimeter site p_{PS} , $P_g(p_{PS})$, is proportional to the η th power of the gradient of the Laplace field at the site [10,11], i.e.,

$$P_g(p_{PS}) \sim |\nabla C(p_{PS})|^\eta \quad (1)$$

(for the original DLA model, $\eta = 1$). This means that the

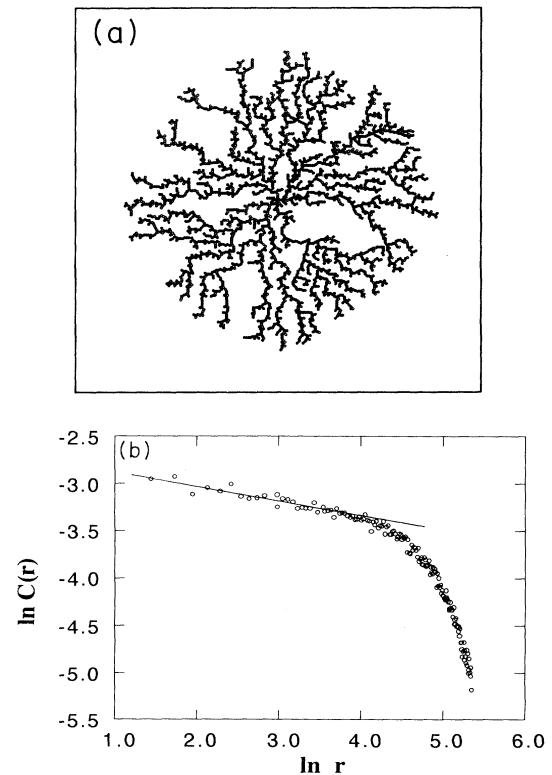


FIG. 4. (a) The cluster generated by the NLA model in computer simulation, with $\lambda = \sqrt{35}$ and $L = 3$ pixel units. (b) The density-density correlation function of the cluster shown in (a); the linear region indicates the scale-invariance property of the NLA cluster.

growth of the fractal is directly governed by the diffusion process. According to Fick's first law, there is no energy barrier in the diffusion process (mass flux is proportional to the solute density gradient). This means that the DLA fractal can grow continuously as long as a solute is diffusing to the interface. In the NLA model, however, the growth of the fractal depends on the random nucleation process. In this case, crystal nuclei are the elementary units of the fractal aggregate. In NLA, the local growth probability at p_{PS} is proportional to the nucleation rate in the solution film [8,9], i.e.,

$$P_g(p_{PS}) \sim \exp\{-\alpha/[\ln(C(p_{PS})/C_0)]^2\} \\ = \exp\{-\alpha/[\ln(\sigma+1)]^2\}, \quad (2)$$

where $C(p_{PS})$ is the concentration at p_{PS} , $\alpha = 4\gamma_{sl}^3\xi^3/27k^3T^3$, and ξ is a geometrical factor of the nuclei. Clearly, the nucleation process is a nonlinear process. It cannot be fully described by the Laplacian

equation, although mass diffusion does influence nucleation. Actually, there exists an energy barrier for nucleation. Only when the local concentration becomes higher than a critical value can the nucleation process occur. That is to say, the NLA fractal may not grow until new nuclei are stimulated somewhere in front of the interface. Therefore we propose that NLA and DLA are different growth models. From Eq. (2) one can find that the supersaturation should be very high in order for the nuclei to be easily stimulated. The NLA actually describes the far-from-equilibrium aggregation process. This growth mechanism may be valid as an alternative to DLA to describe aggregation when the driving force is extremely high and nucleation phenomena are evident.

This work is supported by the grant for key research projects from the State Science and Technology Commission of China.

*Address for correspondence.

- [1] T. Vicsek, *Fractal Growth Phenomena* (World Scientific, Singapore, 1989).
- [2] P. Meakin, in *Phase Transition and Critical Phenomena* (Academic, New York, 1988), Vol. 12, p. 335.
- [3] T. A. Witten and L. M. Sander, *Phys. Rev. Lett.* **47**, 1400 (1981).
- [4] M. Uwaha and Y. Saito, *Phys. Rev. A* **40**, 4716 (1989).
- [5] Mu Wang and Nai-ben Ming, *Phys. Rev. A* **44**, R7898 (1991).
- [6] The details of the surface-tension wave in an extreme situation during the crystal growth, e.g., the oscillation of the aqueous-solution film, have been discussed in Ref. [5].
- [7] O. Söhnel, *J. Cryst. Growth* **57**, 101 (1982); **63**, 174 (1983).
- [8] A. A. Chernov, *Modern Crystallography III* (Springer-Verlag, Berlin, 1984), p. 50.
- [9] Nai-ben Ming, *Fundamentals of the Crystal Growth Physics* (Shanghai Science and Technology, Shanghai, 1982), p. 349. In Chinese.
- [10] M. Matsushita, in *Formation, Dynamics and Statistics of Patterns*, edited by K. Kawasaki, M. Suzuki, and A. Onuki (World Scientific, Singapore, 1990), Vol. 1, p. 158.
- [11] L. Niemeyer, L. Pietronero, and H. J. Wiesmann, *Phys. Rev. Lett.* **52**, 1033 (1984).

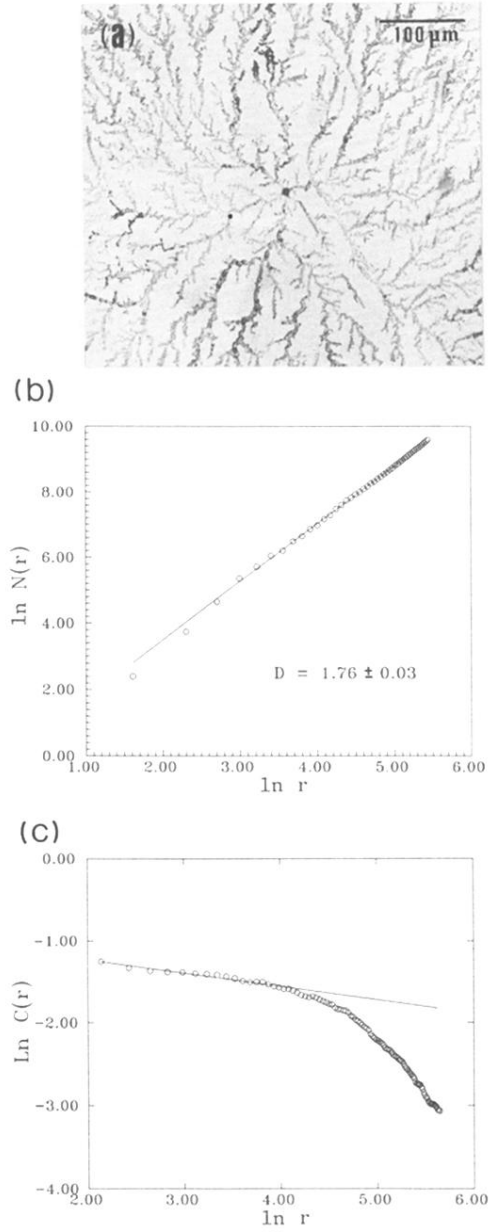


FIG. 1. (a) Typical fractal pattern observed in the experiments. (b) The plot of $\ln N(r)$ vs $\ln r$ to determine Hausdorff dimension of the pattern, where $N(r)$ stands for the area occupied by the fractal within a circle of radius r . (c) The plot to show the density-density correlation function of the cluster shown in (a).

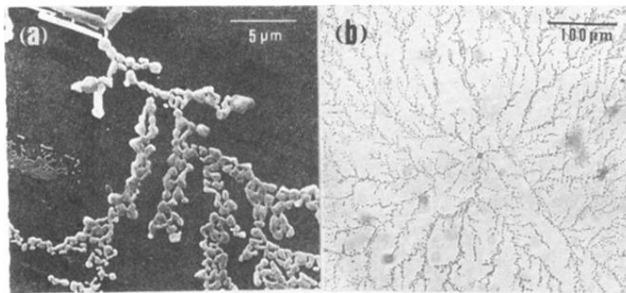


FIG. 2. (a) The fractal branches viewed under a scanning electron microscope. Clearly, the fractal is composed of small crystals. (b) The fractal pattern that has been deliquesced in open atmosphere for several days. The fractal is the same as that shown in Fig. 1(a).

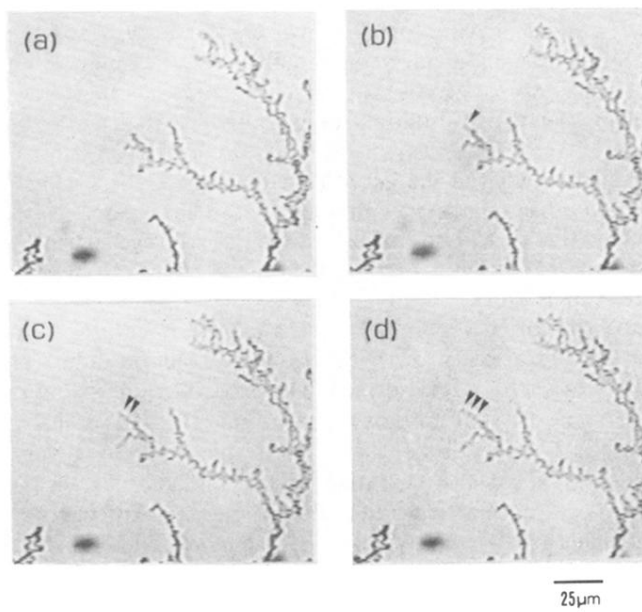


FIG. 3. The fractal-growth process. As indicated by the arrows, successive photos show an additional small crystal generated in front of the tip of the branch. The time interval of two successive photos is about 0.4 s.